Temperature Dependence of Fast and Slow Gating Relaxations of ClC-0 Chloride Channels

Michael Pusch, Uwe Ludewig, and Thomas J. Jentsch

From the Center for Molecular Neurobiology (ZMNH), Hamburg University, D-20246 Hamburg, Germany

ABSTRACT The chloride channel from the *Torpedo* electric organ, ClC-0, is the best studied member of a large gene-family (Jentsch, T.J. 1996. *Curr. Opin. Neurobiol.* 6:303–310.). We investigate the temperature dependence of both the voltage- and chloride-dependent fast gate and of the slow gate of the "double-barreled" ClC-0 expressed in *Xenopus* oocytes. Kinetics of the fast gate exhibit only a moderate temperature dependence with a Q_{10} of 2.2. Steady-state p_{open} of the fast gate is relatively independent of temperature. The slow gate, in contrast, is highly temperature sensitive. Deactivation kinetics at positive voltages are associated with a Q_{10} of ~40. Steady-state open probability of the slow gate ($p_{open}^{slow}(V)$) can be described by a Boltzmann distribution with an apparent gating valence of ≈2 and a variable "offset" at positive voltages. We note a positive correlation of this offset (i.e., the fraction of channels that are not closed by the slow gate) with the amount of expression. This offset is also highly temperature sensitive, being drastically decreased at high temperatures. Paradoxically, the maximum degree of activation of the slow gate also decreases at higher temperatures. The strong temperature dependence of the slow gate was also observed at the single channel level in inside-out patches. The results imply that within a Markovian-type description at least two open and two closed states are needed to describe slow gating. The strong temperature dependence of the slow gate explains the phenotype of several ClC-0 point-mutants described recently by Ludewig et al. (Ludewig, U., T.J. Jentsch, and M. Pusch. 1996. *J. Physiol. (Lond.)*. In press). The large Q_{10} of slow gating kinetics points to a complex rearrangement. This, together with the correlation of the fraction of noninactivating channels with the amount of expression and the fact that the slow gate closes both protochannels simultaneously suggests that the slow gate is coupled to subunit interaction of the multimeric ClC-0 channel.

KEY WORDS: anion channel • multimer • conformational change • double-barrel

INTRODUCTION

ClC proteins represent a large gene-family of voltage-dependent chloride channels (Jentsch et al., 1990; Pusch and Jentsch, 1994; Jentsch et al., 1995*a*; Jentsch, 1996). ClC channels are important for the stabilization of membrane potential in muscle (Steinmeyer et al., 1991*a*) and probably nerve cells (Smith et al., 1995). The importance of the muscular ClC-1 channel (Steinmeyer et al., 1991*b*) is underscored by its involvement in recessive and dominant myotonia (Steinmeyer et al., 1991*a*; Koch et al., 1992; Steinmeyer et al 1994; for review see Jentsch et al., 1995*b*). Mutations in the recently cloned homolog ClC-5 (Fisher et al., 1994; Steinmeyer et al., 1995) are responsible for Dent's disease, a hereditary kidney stone disease with associated proteinuria and hypercalciuria (Lloyd et al., 1996).

The best characterized member of the ClC family is the voltage-gated chloride channel from *Torpedo* electric organ (ClC-0, Jentsch et al., 1990). Its function in the electric organ is to keep the membrane potential close to the chloride equilibrium potential, similar to the function of ClC-1 in skeletal muscle. ClC-0 serves as a model channel for other ClC channels because it can be easily expressed in *Xenopus* oocytes, and its functional characteristics, like voltage dependence and single channel conductance, can be easily measured. Results obtained for ClC-0 are valuable also for other ClC-channels as basic mechanisms of gating and conductance are probably similar in other ClC channels.

The voltage dependence of ClC-0 is characterized by two gates with opposite voltage dependencies. The fast gate operates on single "protochannels" of the "double-barreled" channel (Miller, 1982; Bauer et al., 1991) and opens at depolarized voltages with an apparent gating-valence of ~1. Gating relaxations are in the millisecond time range. The slow gate, on the other hand, opens at negative voltages within seconds, and, once open, closes even more slowly at positive voltages (Pusch et al., 1995*a*; Ludewig et al., 1996*a*).

The fast gating of ClC-0 is strongly dependent on extracellular chloride concentration and recent structure-function studies on ClC-0 established a gating model for the fast gating process that is fundamentally different from the mechanisms proposed for voltage-dependent cation channels (Pusch et al., 1995*a*). In this model, the voltage dependence is conferred by the

Address correspondence to Michael Pusch, Center for Molecular Neurobiology (ZMNH), Hamburg University, Martinistrasse 52, D-20246 Hamburg, Germany. Fax: 49-40-4717-4839; E-mail: pusch@uke.uni-hamburg.de

voltage-dependent binding of the extracellular permeant anion, and not by the movement of an intrinsic voltage sensor. The actual conformational change leading to the opening of the channel is favored if the permeant anion is bound inside the channel. This model accounts for several findings on the fast gating of ClC-0 (Pusch et al., 1995*a*).

Based on effects of internal pH on fast gating of the muscular channel ClC-1, the closing of the channel was proposed to be caused by a block by internal OH^- ions (Rychkov et al., 1996). In this model, voltage-dependent binding of external chloride leads to a lowering of the binding affinity of the blocking OH^- ion, and thus to channel opening. Such a mechanism is consistent with the leftward shift of the open probability ($p_{open}(V)$)[1]-curve observed with lowered internal pH (Rychkov et al., 1996). An allosteric modulation by internal OH^- (or H^+) of a conformational transition associated with channel opening could, however, not be completely ruled out. Also, the experiments performed by Hanke and Miller on the pH dependence of ClC-0 in lipid bilayers (Hanke and Miller, 1983) argue against such a simple blocking mechanism.

We decided to measure the temperature dependence of the fast gating process in ClC-0 in order to get more insight into its mechanism. Different temperature dependencies would be expected for a simple, possibly diffusion-limited blocking process, and an open-closed transition caused by a conformational change of the protein.

Little is known yet about the mechanism of the slow gate. Within the double-barreled model (Miller, 1982), the slow gate closes both protochannels simultaneously at positive voltages. It is well established that ClC channels are multimers (Middleton et al., 1994; Steinmeyer et al., 1994). Recent experiments strongly suggest a dimeric structure for ClC-0 (Ludewig et al., 1996*b*; Middleton et al., 1996). If each protochannel of ClC-0 consists of one subunit, it is conceivable that the slow gate is linked to subunit-interaction. Recent mutagenesis data of ClC-0 (Ludewig et al., 1996*a*) identified several amino acids in a conserved stretch of amino acids close to lysine 519 that drastically accelerated the closing of the slow gate. Some mutations also led to a slowed kinetics.

Here, we measure the temperature dependence of the slow gate and find a huge temperature coefficient of the gating relaxations and a strong dependence of the fraction of channels that can be closed by the slow gate. From these data we conclude that within a simple Markovian-type description the slow gate involves at least two open and two closed states. We also find a dependence of the slow gate on the amount of expression. This, together with the large temperature dependence make it likely that the slow gate is involved in subunit interaction.

The phenotype of several point mutations that altered slow gating properties (Ludewig et al., 1996*a*) find an easy explanation from our results on the temperature dependence.

Apart from being a biophysical tool, the temperature dependence may also be of physiological or pathophysiological importance, e.g., for the muscular chloride channel ClC-1, as cooling aggravates myotonic symptoms in some patients (Becker, 1973).

MATERIALS AND METHODS

Molecular Biology and Electrophysiological Measurements

Mutations P522G and L524I have already been described (Ludewig et al., 1996*a*). Briefly, two overlapping PCR products containing both the desired mutation were generated using one mismatch primer for each. The two PCR products were combined together with the external primers, and another PCR was performed. The resulting fragment was cut with appropriate restriction endonucleases and ligated into the expression construct. The constructs were verified by sequencing. Mutant P522G has a drastically accelerated deactivation of the slow gate, whereas mutant L524I shows a more incomplete deactivation of the slow gate at positive voltages. Capped cRNA was transcribed in vitro using the mMessage mMachine kit (Ambion Inc., Austin TX). *Xenopus* oocytes were prepared, injected, handled, and voltage-clamped with two microelectrodes as described (Pusch et al., 1995*b*). The recording solution in two-microelectrode voltage-clamp was ND96 (Pusch et al., 1995*b*). Temperature was measured with a small temperature-sensitive thermoelement close to the oocyte. It was maintained constant (±0.5°K) manually by changing independently the perfusion rate of a room temperature (~20°C), a precooled (~1°C), and a preheated (~50°C) ND96 solution, respectively.

Single channel experiments were performed using the inside-out configuration of the patch-clamp technique (Hamill et al., 1981) on oocytes from which the vitelline membrane had been removed (Methfessel et al., 1986). They were bathed in a solution containing (in mM) 100 NMDG-Cl, 2 $MgCl_2$, 5 HEPES, 5 EGTA, pH 7.4. Pipettes were filled with a solution containing (in mM) 95 NMDG-Cl, 5 $MgCl_2$, 5 HEPES, pH 7.4. In the patch experiments temperature was changed using a Peltier-based bath-temperature controller (Luigs and Neumann, Ratingen, Germany) and measured as in two-microelectrode experiments.

Pulse Protocols and Data Analysis

Raw data were analyzed with home-written software and were then further processed using the SigmaPlot program (Jandel Scientific, Corte Madera, CA).

Steady-state (apparent) open probability of the fast gate ($p^{fast}_{open}(V)$) was obtained as described earlier (Pusch et al., 1995*a*). Briefly, first the slow gate was opened by a hyperpolarizing pulse. Once open it stays open for at least several seconds. Then, the fast gate was driven into steady state at various potentials. The degree of fast-activation was monitored at a constant test-pulse of −100 mV. At −100 mV fast gating relaxations are relatively slow (τ_{fast}[−100 mV] ~ 10 ms at room temperature) such that a reliable extrapolation of the current to the onset of the test pulse is

[1]*Abbreviations used in this paper:* p_{open}, open probability; Q_{10}, temperature coefficient; WT, wild type.

possible. The peak currents at the constant test potentials were normalized by the maximal value and plotted versus the conditioning voltage. The resulting p_{open}^{fast} was fitted by Boltzmann distributions of the form $p_{open}^{fast}(V) = p_o + (1 - p_o)/(1 + \exp\{z^{fast}F[V_{1/2}^{fast} - V)/RT]\}$ with an "offset" p_o (Ludewig et al., 1996*a*), where R is the gas constant, F is the Faraday constant, T is the temperature (in Kelvin), $V_{1/2}^{fast}$ is the voltage where the Boltzmann term is 0.5 and z^{fast} is the apparent gating valence.

The time course of deactivating fast gating relaxations at hyperpolarized voltages was fitted with a single exponential function.

Deactivation of the slow gate was measured using a home-written slow-acquisition/stimulation program (CHART). To avoid excessive chloride movements, deactivation of the slow gate was measured at −30 mV, a value that is close to the reversal potential. To monitor the degree of activation of the slow gate, the potential was stepped repeatedly to +40 mV for brief periods. The previous activation of the slow gate by stepping the potential to −120 or −140 mV for several seconds (not shown in Fig. 3) sometimes led to a transient shift of the reversal potential due to net chloride movement. This explains the current relaxations seen at −30 mV in Fig. 3 *A* (24.6°C). This relaxation has no relationship with the slow gate.

Steady-state (apparent) open probability of the slow gate ($p_{open}^{slow}(V)$) was obtained using the pulse-protocol shown in Fig. 4 *A*. To compare the absolute current amplitudes at different temperatures, values were not normalized. $p_{open}^{slow}(V)$ could be fitted by a Boltzmann function of the form:

$$p_{open}^{slow} = I_{max}\{f_{ni} + (1 - f_{ni})/(1 + \exp[-z^{slow}F(V_{1/2}^{slow} - V)/RT])\},$$

where I_{max} is the (extrapolated) current at +40 mV measured after maximal activation of the slow gate. f_{ni} represents the fraction of channels that are not inactivated by the slow gate at positive voltages. The other symbols have a similar meaning as above.

In patch-experiments the slow gate was monitored using the following pulse protocol. The patch was held at the desired holding potential at which the slow gate was to be studied. Every 1–3 s a brief (50 ms) pulse was given to +60 mV. At +60 mV the fast gate opens within <1 ms and therefore the average current at +60 mV reflects the number of channels with an open slow (and fast) gate. If only a few channels are present in the patch, their number can be easily counted. In addition, the brief exposures to +60 mV did not significantly change the status of the slow-gate activation because the gating-time constant at positive voltages is in the order of at least several seconds.

Temperature coefficients (Q_{10}) and (apparent) activation enthalpies ($\Delta H^{\ddagger}$) were extracted from the data using the Arrhenius equation:

$$k(T) = (A/T) \cdot \exp(-\Delta H^{\ddagger}/[RT]),$$

where k is a rate constant at the temperature T, R is the gas constant, and A is a constant factor. The same equation was applied for the analysis of time constants even if it is not strictly valid in this case. The Q_{10} was calculated from $\Delta H^{\ddagger}$ according to $Q_{10} = k(T + 10K)/k(T)$ for $T = 293$°K.

RESULTS

Temperature Dependence of the Fast Gate in Wild-type (WT) ClC-0

As expected, closing of the fast gate is slowed at low temperatures and accelerated at high temperatures (Fig. 1, *A* and *C*). Relaxations are too fast to be resolved at T > 30°C. Steady-state voltage dependence, on the other hand, is almost independent of temperature (Fig. 1 *B*). The voltage of half-maximal activation, $V_{1/2}^{fast}$, varies by only 7 mV in the T range from 8.7–24.3°C. Quantitative analysis of the temperature dependence of deactivation time constants yields an almost voltage-independent activation enthalpy of 51 kJ/mole, corresponding to a Q_{10} value of 2.2 (Fig. 1 *C*). This value is significantly larger than a Q_{10} that is typical for diffusion (i.e., 1.3–1.6). Relaxations are monoexponential at all temperatures consistent with a simple apparent two-state system (Hanke and Miller, 1983; Pusch et al., 1995*a*).

Fast gating is slowed about twofold when extracellular chloride is partially replaced by iodide (Fig. 2 *A*; compare Figs. 1 *C* and 2 *B*). This slowing could be accompanied by a changed temperature dependence of fast gating. However, the activation enthalpy derived from the relaxations in solutions with 80 mM chloride replaced by iodide is ~49 kJ/mole (Fig. 2 *B*), a value not statistically different from that obtained in pure chloride.

Temperature Dependence of the Deactivation of the Slow Gate

Activation-kinetics of slow gating are difficult to measure at negative voltages due to the simultaneous closure of the fast gate. Therefore, we concentrated on the deactivation at depolarized voltages. Closing of the slow gate at a holding potential of −30 mV can be monitored by repetitive short pulses to +40 mV (Fig. 3 *A*). The time course of closing can be nicely fitted by a single exponential function with a time constant of ~300 s at room temperature (Ludewig et al., 1996*a*). This closing kinetics shows a dramatic temperature dependence (Fig. 3, *A* and *B*). The apparent activation enthalpy is 260 kJ/mole, corresponding to a Q_{10} of ~40 at 20°C. Such a large temperature dependence is not easily compatible with a simple conformational change.

Incomplete Closure of the Slow Gate at Positive Voltages

Our usual protocol to measure the steady-state activation of the slow gate is shown in Fig. 4 *A*. The slow gate is progressively opened by a 7-s conditioning pulse and the degree of activation is then measured at the +40 mV test-pulse. At this voltage the fast gate is maximally open. The direction of the protocol (i.e., from positive to negative voltages) is important because of the slow deactivation time course of the slow gate (see above). Plotting the current measured at the 40-mV test-pulse versus the conditioning voltage for WT ClC-0 yields the values shown as circles in Fig. 4 *E*. It can be seen that the slow gate starts to activate at negative voltages. The activation can be described by a Boltzmann fit with a $V_{1/2} \sim -80$ mV. Another important aspect is that the slow gate apparently does not deactivate completely at

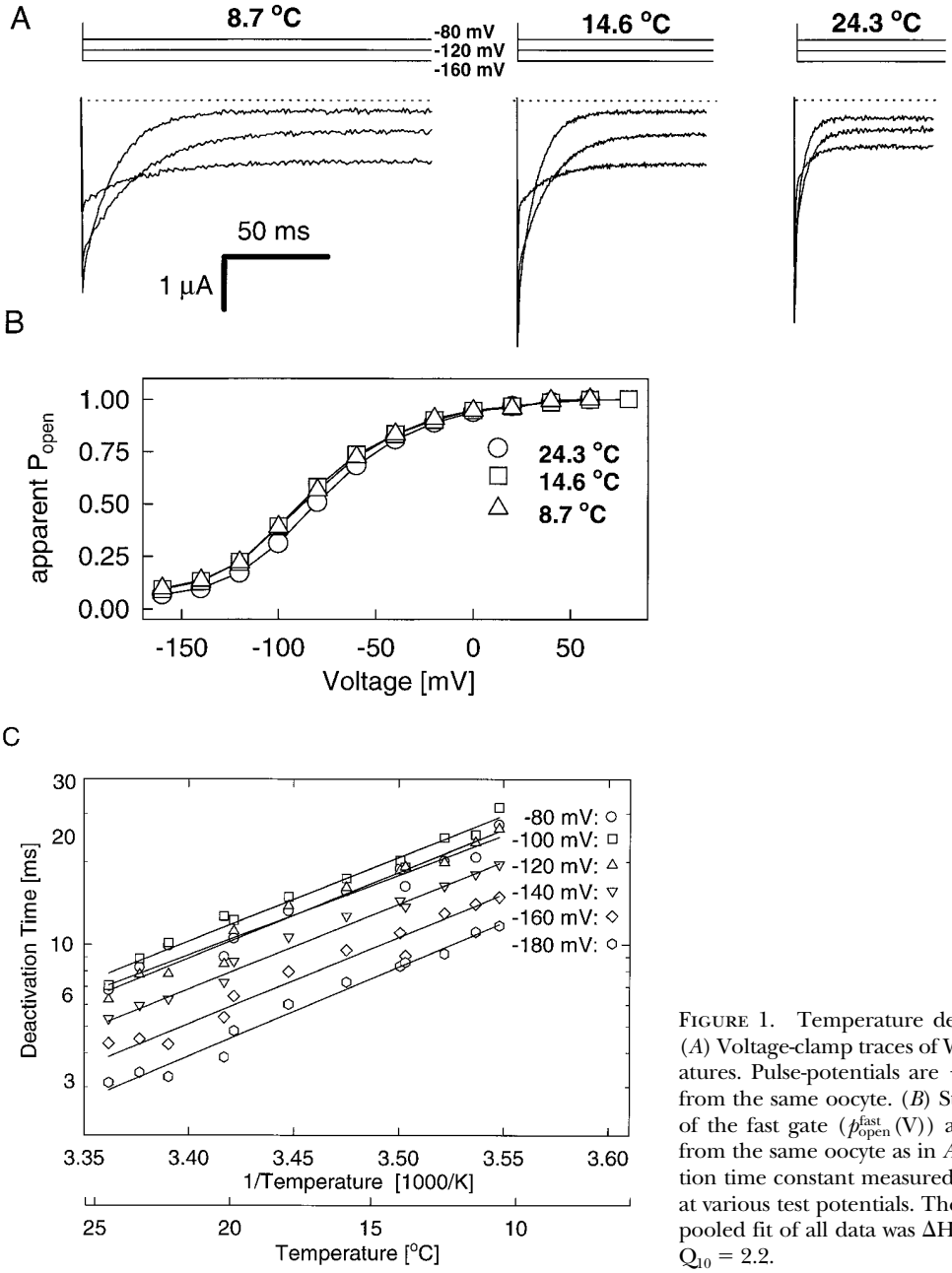

FIGURE 1. Temperature dependence of fast gate of WT ClC-0. (*A*) Voltage-clamp traces of WT ClC-0 measured at various temperatures. Pulse-potentials are −160, −120, and −80 mV. Data are from the same oocyte. (*B*) Steady state apparent open probability of the fast gate (p_{open}^{fast}(V)) at three different temperatures (data from the same oocyte as in *A*). (*C*) Arrhenius plot of the deactivation time constant measured from the same oocyte as in *A* and *B*, at various test potentials. The activation enthalpy obtained from a pooled fit of all data was $\Delta H^{\ddagger} = 51 \pm 2$ kJ/mol corresponding to $Q_{10} = 2.2$.

positive voltages, leading to an offset of p_{open}^{slow}(V) at positive voltages. This offset is clearly due to heterologously expressed ClC-0 channels. Noninjected oocytes had consistently smaller currents (Fig. 4 *C*). Additionally, outward currents through ClC-0 channels can be almost completely blocked by applying extracellular iodide, in contrast to endogenous oocyte currents (data not shown). This allowed a clear distinction between endogenous currents and currents through ClC-0 channels.

An important question is whether or not the offset is artifactually introduced because the conditioning pulse of the protocol (Fig. 4 *A*) is too short to drive the slow gate into steady state. To test for this possibility we applied the pulse protocol with much longer conditioning pulses (84 s) on the same oocyte (Fig. 4 *D*). The resulting p_{open} is shown in Fig. 4 *E* as squares. The form of the p_{open}(V) is slightly different from the experiment obtained from the shorter prepulses. This could be due to unspecific drifts or slow changes in the local chloride concentrations during the extremely long pulses. Most importantly, however, it is clear that the slow gate does not deactivate further at positive voltages. Additional evidence for the presence of such an offset is shown in the continuous recording from the same oocyte (Fig. 4 *F*). After activating the slow gate at −120 mV (not shown) deactivation was first monitored at a holding

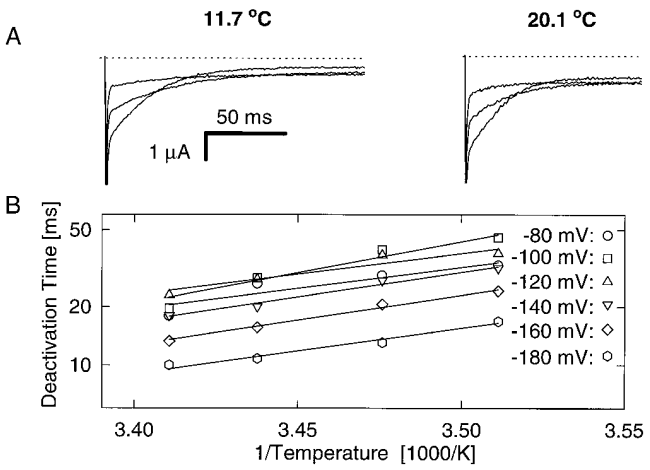

FIGURE 2. Temperature dependence of deactivation time constants in 80 mM iodide. (*A*) Voltage-clamp traces measured from a WT ClC-0 expressing oocyte in a solution with 80 mM extracellular chloride replaced by iodide at two different temperatures. The "spikes" that are seen immediately after the voltage step are caused by the capacitive transient. (*B*) Arrhenius plot of the deactivation time constants. A fit to the Arrhenius equation yields $\Delta H^{\ddagger} = 49 \pm 3$ kJ/mol corresponding to $Q_{10} = 2.1$.

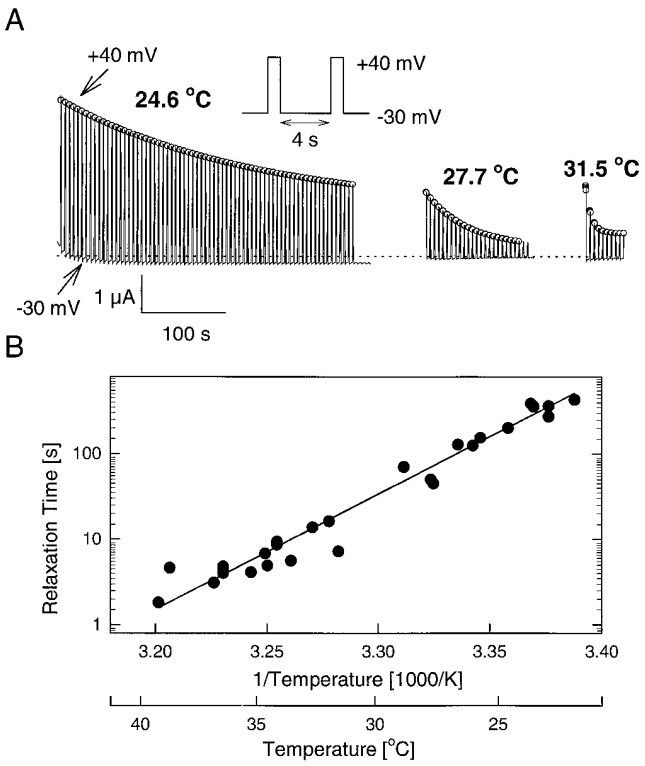

FIGURE 3. Temperature dependence of slow gate deactivation. (*A*) After maximal activation of the slow gate at −140 mV for ~10 s (not shown), deactivation was monitored by repetitive pulse to +40 mV from a holding potential of −30 mV (*inset*). The fast apparent relaxation seen for the current at −30 mV at 24.6°C is due to a drift of the reversal potential caused by the previous hyperpolarization. It has no relationship to the slow gate. Data are from the same oocyte. Superimposed (*circles*) are shown single exponential fits to the deactivation time course with the time constants 230 s (24.6°C), 50 s (27.7°C), and 6.9 s (31.5°C). (*B*) Arrhenius plot of deactivation time constants of the slow gate pooled from several oocytes. The line shows a fit of the Arrhenius equation yielding $\Delta H^{\ddagger} = 260$ kJ/mol.

potential of −30 mV. After reaching steady state, the holding potential was switched to 0 mV. This does, however, not lead to a further deactivation. Now, after a brief activation of the slow gate by switching to V_{hold} to −120 mV, deactivation at $V_{hold} = 0$ mV is only slightly slower ($\tau = 108$ s) than at $V_{hold} = -30$ mV ($\tau = 77$ s). Then, switching again to $V_{hold} = -30$ mV does not lead to an activation. Thus, from these experiments we can conclude that the slow gate does not fully close at positive potentials. A certain fraction of channels is not inactivated even at depolarized potentials.

Correlation of the Fraction of Noninactivating Channels with the Expression Level

In the course of this study we noted a certain variability of the fraction of noninactivating channels from oocyte to oocyte, with the tendency of a larger offset with higher degrees of expression. To study this systematically we measured several oocytes from the same batch that had been injected with various amounts of RNA. Temperature was kept constant at 22.5°C. The results are shown in Fig. 5. It can be seen that the offset correlates positively with the amount of expression of ClC-0 channels in the oocyte. With increasing expression the offset increases from ~15 to ~50% for the maximally expressing oocytes.

Temperature Dependence of the Steady-state Open Probability of the Slow Gate

To measure the temperature dependence of the steady state activation of the slow gate we used the protocol shown in Fig. 4 *A* to avoid the technical difficulties associated with the extremely long prepulses that are necessary to get a real steady state at positive voltages. As shown above, the steady state is saturated at voltages >−30 mV, and the current does not deactivate further. The time constants at more negative voltages are small enough to get a reasonable estimate of the steady state using the short pulse-protocol. The $p_{open}^{slow}(V)$ thus obtained (Fig. 6 *B*) can be fitted by a Boltzmann distribution with a variable offset (see MATERIALS AND METHODS). Temperature strongly affects this fraction on noninactivating channels. Increasing the temperature, leads to a decrease of the offset component to <14% at 37°C (Fig. 6 *B*). On the other hand, the maximal current obtained after stimulation of the slow gate at −140 mV also decreases in a paradoxical fashion above 30°C (Fig. 6, *A* and *B*), even though single channel current increases at higher temperatures (see below). Thus,

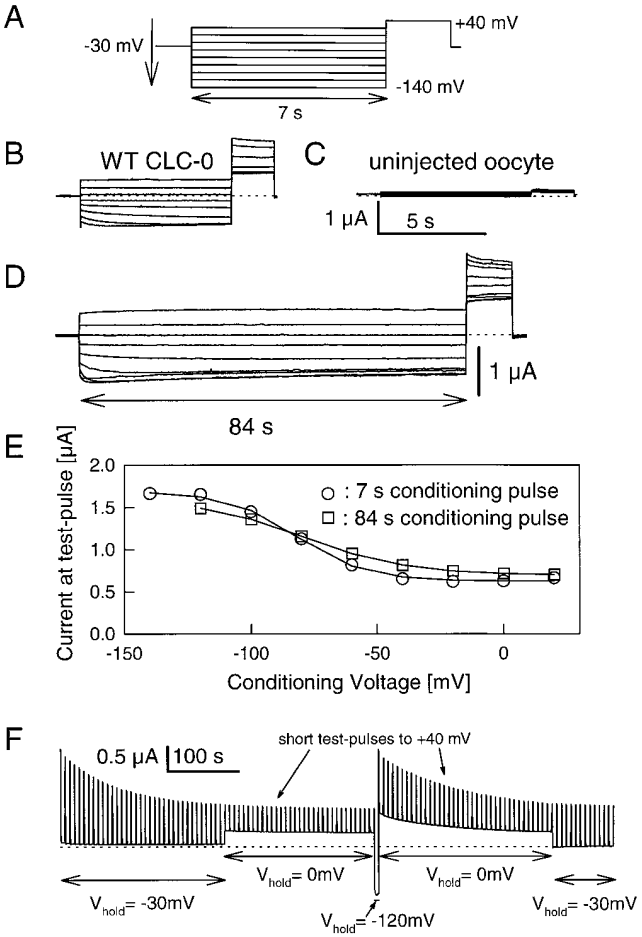

FIGURE 4. Incomplete deactivation of the slow gate at positive voltages. (*A*) Usual pulse protocol to measure $p_{open}^{slow}(V)$. The slow gate was progressively opened with 7-s pulses from +20 to −140 mV. The degree of the activation was monitored at the constant "tail" potential of +40 mV. (*B*) Family of currents obtained by the protocol shown in *A* from a ClC-0 expressing oocyte. (*C*) Currents from a noninjected oocyte from the same batch. (*D*) Currents from the same oocyte as shown in *B* using a longer prepulse (84 s). (*E*) I-V relationships obtained from the currents shown in *B* (*circles*) and *D* (*squares*). Solid lines are Boltzmann fits with $V_{1/2} = -82$ mV (*circles*) and $V_{1/2} = -79$ mV (*squares*). (*F*) Continuous recording (same oocyte as *B* and *D*). Before the start of the recording the voltage had been clamped to −120 mV for several seconds to activate the slow gate. The holding potential was varied as indicated. The small "blips" represent the currents measured during brief steps to +40 mV to monitor the degree of the slow gate activation. Temperature was 28°C for the experiments shown in *B*, *D*, *E*, and *F*.

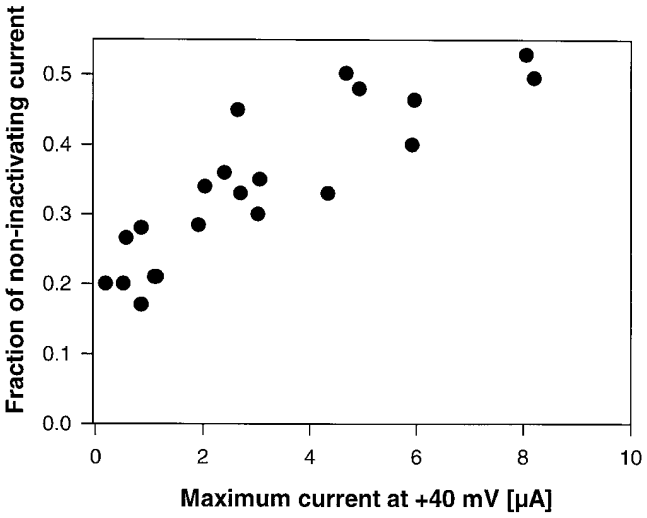

FIGURE 5. Correlation of the fraction of noninactivating channels with the amount of expression. In a batch of oocytes injected with various amounts of cRNA to obtain a varying degree of expression, slow-gate activation was measured at 22.5°C as in Fig. 4, *A* and *E*. The offset of the Boltzmann-fit, i.e. the fraction of noninactivating channels, is plotted versus the maximal activation (offset is relative to the maximum).

high temperature leads to a more complete inactivation of channels at more positive voltages and to a decrease in the fraction of channels that can be activated by the slow gate at negative voltages. The mid-voltage of half-maximal activation, $V_{1/2}^{slow}$, is relatively independent of temperature (see legend to Fig. 6 *B*).

The decrease of currents at higher temperature is clearly an effect on slow gating (as opposed to effects on fast gating or on single channel amplitude) as is best illustrated in the continuous recording shown in Fig. 7 (temperature-clamp). It can be seen that at the constant holding potential of −30 mV a quick increase of temperature from 23 to 33°C (*left arrow*, Fig. 7) first leads to an immediate slight increase of the current. This is probably due to the instantaneous effect on the single channel amplitude (see below). Afterwards, at constant temperature of 33°C, the current decreases with a time constant of ~40 s to a new steady-state value. Similarly, now a decrease of temperature to 25°C leads to an instantaneous decrease of current (*right arrow*, Fig. 7) and a much slower increase of the current with a time constant of 200 s.

Single Channel Analysis of Temperature Effects on Slow Gating

The macroscopic measurements of the slow gate leave some uncertainties because effects of temperature on the single channel current amplitude are not controlled and because no absolute but only relative open probabilities can be assessed. Therefore we sought to measure the effect of temperature on the slow gate at the single channel level. Fig. 8, *A* and *B*, show continuous recordings of inside-out patches containing only a few channels at a holding potential of −140 mV (Fig. 8 *A*) and of 0 mV (Fig. 8 *B*). The upper traces show the current measured during brief pulses to +60 mV. The brief pulses to a positive voltage do not change significantly the state of the slow gate (see above). Because

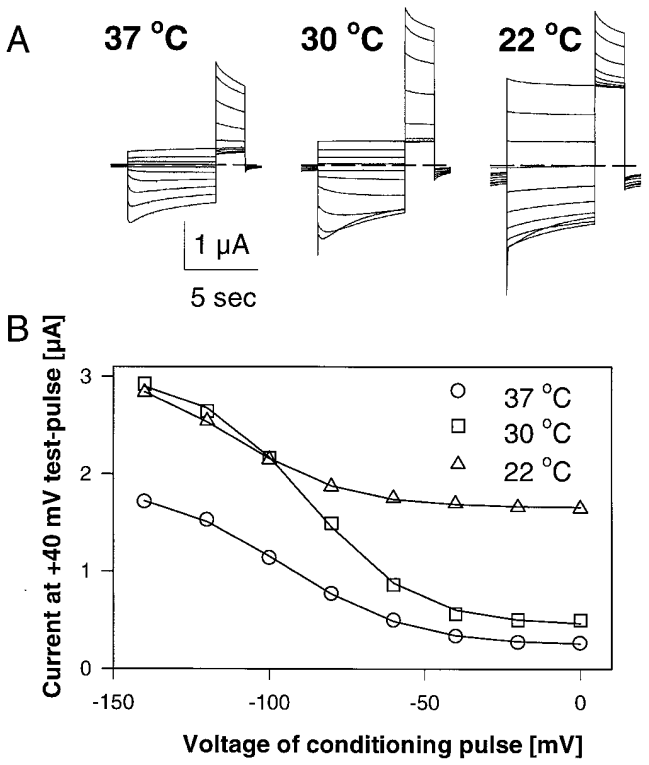

FIGURE 6. Temperature dependence of steady-state $p_{open}^{slow}(V)$. (*A*) Family of voltage-clamp traces measured from the same oocyte at the indicated temperatures. (*B*) Steady-state $p_{open}^{slow}(V)$ measured as the current response at the tail potential (40 mV) after the 7-s conditioning pulse obtained from the data shown in *A*. Note that the current response at +40 mV is additionally influenced by the effect of the temperature on the single channel current. Solid lines represent Boltzmann-fits (half-maximal voltage is $V_{1/2} = -112$ mV at 22°C, −88 mV at 30°C, −95 mV at 37°C).

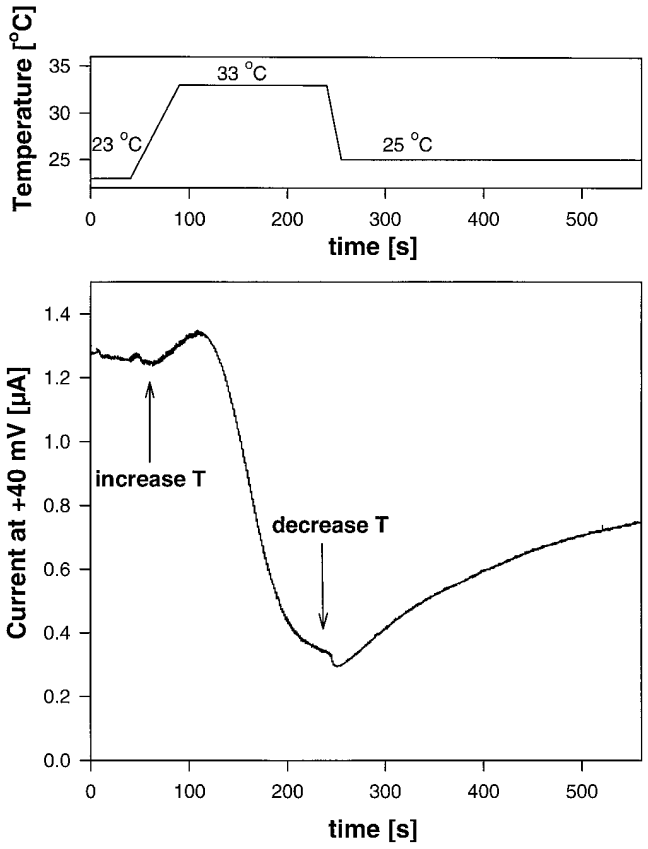

FIGURE 7. Continuous recording of slow gate at constant voltage. A continuous recording (see Fig. 3) is shown. Only the current recorded at +40 mV is displayed as a continuous trace. In the upper trace the temperature time course is shown. The temperature was suddenly shifted from ≈23°C to ≈33°C (*up arrow*). After ≈200 s it was decreased again to ≈25°C (*down arrow*). The holding potential was −30 mV.

the fast gate of both protochannels is almost completely open at +60 mV, the current at this voltage reflects the number of channels with an open slow gate. This number can be directly counted for the experiments shown in Fig. 8, *A* and *B*, and the result is shown in the middle traces. The temperature was changed during the experiment as shown in the lower traces. It can be clearly seen that at −140 mV (Fig. 8 *A*) at the lower temperatures (<18°C) two channels are almost constantly open. Assuming a total number of two channels in the patch, the open probability at T < 18°C is $p_{open}^{slow} = 0.97$. Increasing the temperature leads to an increase of the single channel current (upper trace). But, most importantly, the frequency of closures of the slow gate increases dramatically leading to a steady-state value of p_{open}^{slow} of 0.82 at 24°C. The results are similar at a holding potential of 0 mV (Fig. 8 *B*), although the experiments are more difficult to perform because the gating transitions of the slow gate are extremely slow at 0 mV and temperatures below 20°C (see above). The qualitative effect of an increase in p_{open}^{slow} during cooling is, however, clearly visible.

From these experiments the dependence of the single channel current amplitude on temperature can also be measured. Fig. 9 shows the dependence for the current at −140 mV (*squares*) and the current at +60 mV (*circles*). As expected, single channel current increases with increasing temperature. The solid lines correspond to a Q_{10} of ~1.4, even though the dependence cannot be well described by the Arrhenius equation. The shallow temperature dependence is, however, consistent with a diffusion process.

A Markov Type Model of the Slow Gate Requires at least Four States

The temperature dependence of $p_{open}^{slow}(V)$ cannot be explained by a simple two state mechanism with standard voltage-dependent rate constants. Also, more than one open state is needed to explain the temperature

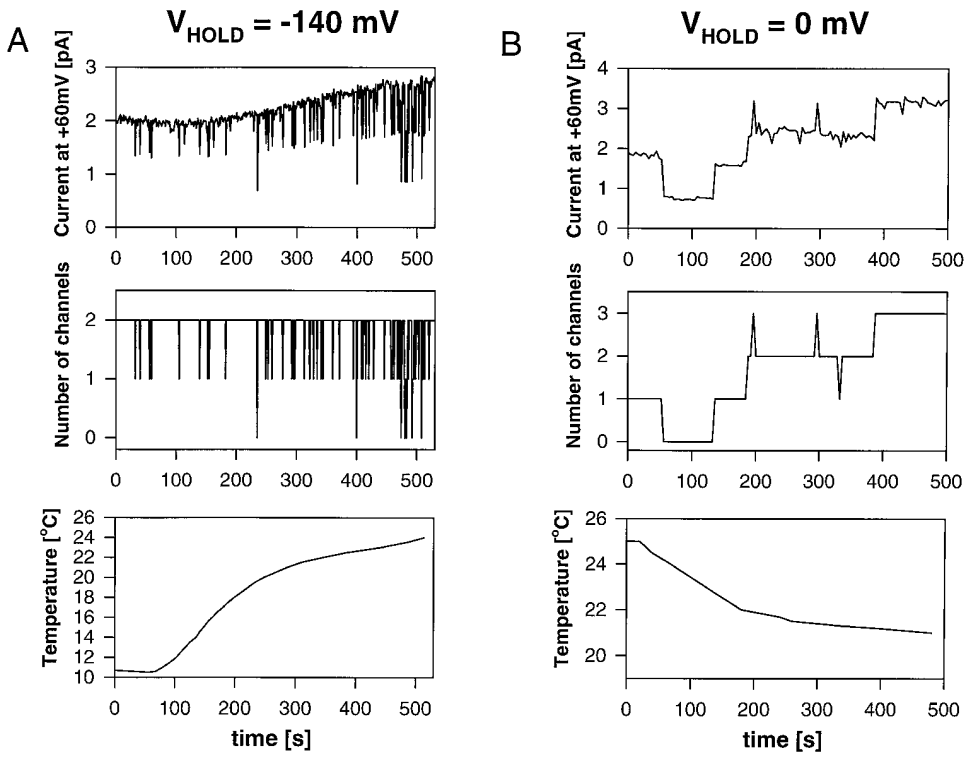

FIGURE 8. Effects of temperature on slow gating at the single channel level. Activation of the slow gate was recorded as described in MATERIALS AND METHODS. Inside-out patches were held at the indicated voltages. Every 1 to 2 s a brief (50 ms) pulse to +60 mV was applied. The current measured during this period is displayed in the upper panels (*A* and *B*) (no leak subtracted). The number of channels that are open during the 50-ms test pulse can be easily counted (*middle traces*, *A* and *B*).

dependent offset of steady-state $p_{open}^{slow}(V)$ (see DISCUSSION). A minimal model consisting of four states that is able to describe the temperature and voltage dependence of the slow gate is illustrated in Fig. 10 *E*. Two open states and two closed states are connected among each other by voltage-dependent rates. The temperature-dependent step connects open and closed states. This arrangement of states leads to a saturation of $p_{open}^{slow}(V)$ at extreme positive or negative voltages at values different from 0 or 1, respectively. These saturating values of p_{open}^{slow} are modulated by the temperature dependent steps.

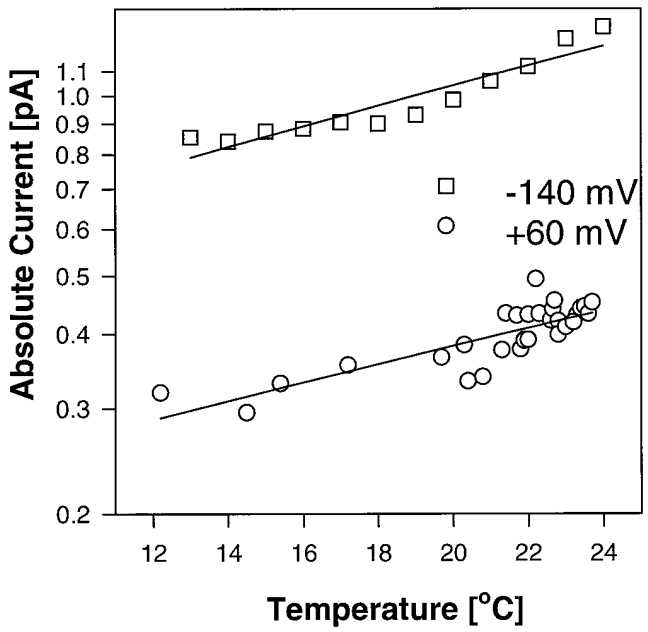

FIGURE 9. Dependence of the single channel current on temperature. From the experiments shown in Fig. 8, the single channel amplitude was measured and plotted versus the temperature. Solid lines represent Arrhenius-fits yielding Q_{10} = 1.4.

Mutants with Altered Slow Gate

Several ClC-0 mutants with altered properties of the slow gate have been described recently (Ludewig et al., 1996*a*). Some of the mutants showed an acceleration of deactivation, whereas others were characterized by an increased fraction of noninactivating current. As shown above, these phenotypes resemble WT behavior at increased or decreased temperature, respectively. Therefore, we sought to analyze the temperature dependence of the slow gate of some of the mutations. P522G shows a drastically accelerated and more complete deactivation of the slow gate, whereas L524I, in contrast, showed incomplete deactivation (Ludewig et al., 1996*a*; Fig. 11 *B*). Fig. 11 *A* illustrates that the phenotype of mutant P522G can be made similar to WT by cooling the oocyte by some degrees. By analogy, the fraction of noninactivating channels can be reduced for mutant L524I by heating such that steady-state p_{open}^{slow} looks similar to that of WT (Fig. 11 *B*).

These results are qualitatively understandable within the framework of the slow gate model described above.

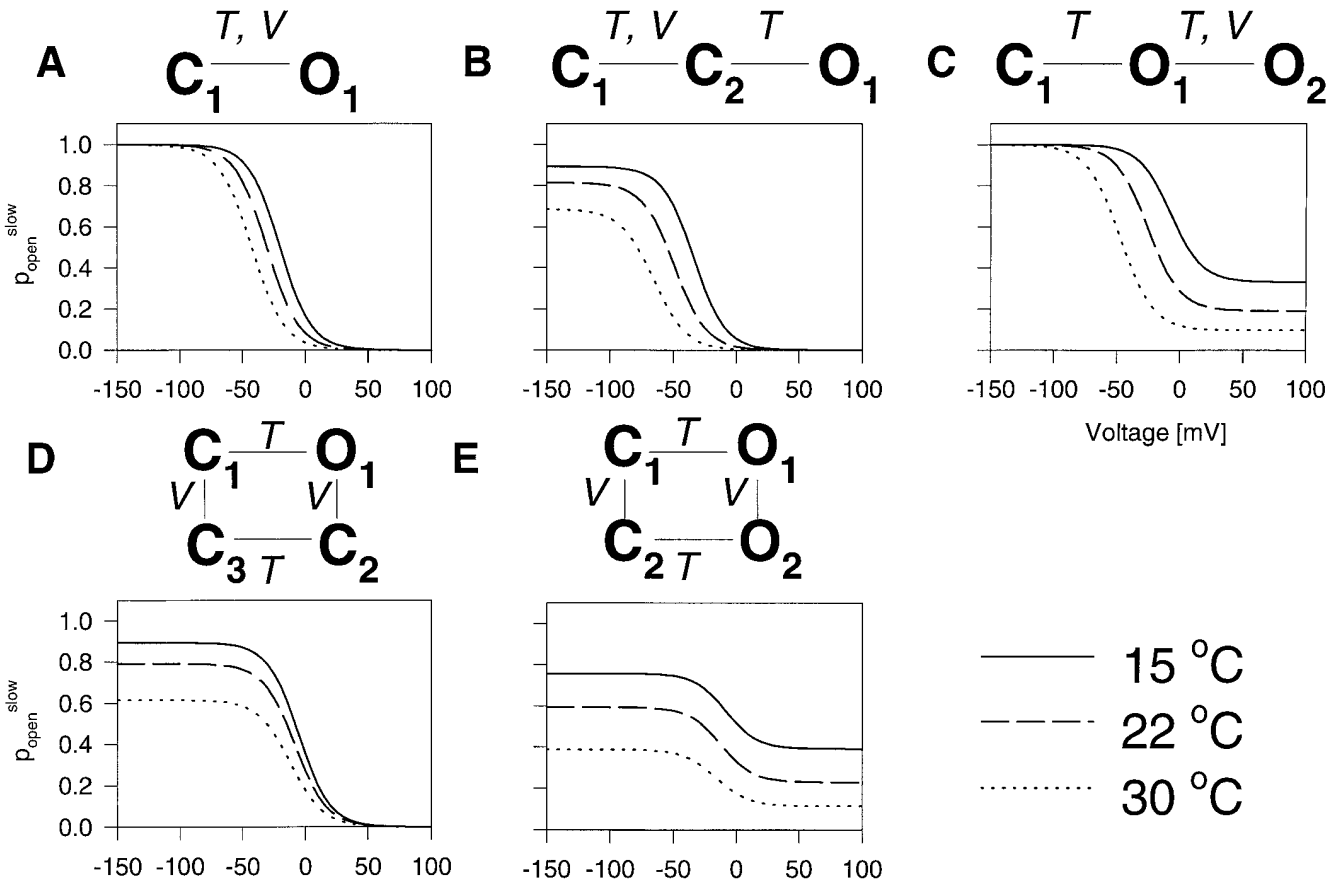

FIGURE 10. Necessity of a four-state model to describe the slow gate. Several models with two, three, or four states were tested for the ability to reproduce the temperature dependence of steady-state $p_{open}^{slow}(V)$ found for ClC-0, as shown in Fig. 6. The states are assumed to be in equilibrium such that microscopic reversibility applies. The ratio of occupation probability of two states, *A* and *B*, is assumed to be of the form:

$$p_A/p_B = \exp[(-\Delta G_A + \Delta G_B)/RT] = \exp(-\Delta G_{AB}/RT) = \exp(\Delta S_{AB}/R - \Delta H_{AB}/RT + z_{AB}VF/RT),$$

where *G* is the Gibbs free energy, *S* the entropy, *H* the enthalpy, *R* the gas constant, *T* the (absolute) temperature, *F* the Faraday constant, and *V* the membrane voltage. The "gating valence," z_{AB}, describes the voltage dependence of the transition A ↔ B. Assuming certain values for S_i, H_i, and z_{ij} for the various states, the steady-state $p_{open}(V)$ curves were calculated for each model for three different temperatures as indicated. Temperature-sensitive steps (i.e., $\Delta H_{AB} \neq 0$) are indicated by a *T*, voltage-dependent steps (i.e., $z_{AB} \neq 0$) are indicated by *V*. The predictions of the models have to be compared (qualitatively) with the data shown in Fig. 6 *B*, keeping in mind, however, that the absolute current amplitude plotted in Fig. 6 is additionally dependent on temperature via the dependence of the single channel amplitude. Clearly, a two-state model (*A*) incorporating some voltage dependence can be ruled out because p_{open} tends to 0 at high voltages and approaches 1 at negative voltages, irrespective of *T*. For both three-state models (*B* and *C*) the same holds true either at high or at low voltages, no matter how voltage or temperature dependence is assigned to the various transitions. A four-state model with only one open state and at least one voltage-dependent transition (*D*) leads also to a $p_{open}(V)$ that tends to either 0 or 1 either at high or at low voltages. Thus, the minimal model that is actually able to qualitatively account for the voltage and temperature dependence is the one shown in *E*. Interestingly, the voltage-dependent transitions are not the ones connecting open and closed states but rather the open and two closed states respectively. Parameters for the simulation are (ΔH in kJ/mol, ΔS in kJ/mol/K) (*a*) $\Delta H_{C1O1} = 80$, $\Delta S_{C1O1} = 0.29$, $z_{C1O1} = 2$; (*b*) $\Delta H_{C1C2} = 60$, $\Delta S_{C1C2} = 0.25$, $z_{C1C2} = 2$, $\Delta H_{C2O1} = 65$, $\Delta S_{C2O1} = 0.21$, $z_{C2O1} = 0$; (*c*) $\Delta H_{C1O1} = 75$, $\Delta S_{C1O1} = 0.27$, $z_{C1O1} = 0$, $\Delta H_{O1O2} = 80$, $\Delta S_{O1O2} = 0.29$, $z_{O1O2} = 2$; (*d*) $\Delta H_{C1O1} = 80$, $\Delta S_{C1O1} = 0.26$, $z_{C1O1} = 0$, $\Delta H_{O1C2} = 0$, $\Delta S_{O1C2} = 0$, $z_{O1C2} = -2$, $\Delta H_{C2C3} = -70$, $\Delta S_{C2C3} = -0.24$, $z_{C2C3} = 0$; (*e*) $\Delta H_{C1O1} = 77$, $\Delta S_{C1O1} = 0.26$, $z_{C1O1} = 0$, $\Delta H_{O1O2} = 0$, $\Delta S_{O1O2} = 0$, $z_{C1O1} = -2$, $\Delta H_{O2C2} = -78$, $\Delta S_{O2C2} = -0.27$, $z_{O2C2} = 0$.

The main effect of the mutants is a relatively small change of the activation enthalpy of the conformational transitions and of the enthalpic contribution of the Gibb's free energy of the various states.

DISCUSSION

We analyzed the temperature dependence of fast and slow gating of the *Torpedo* chloride channel ClC-0 and

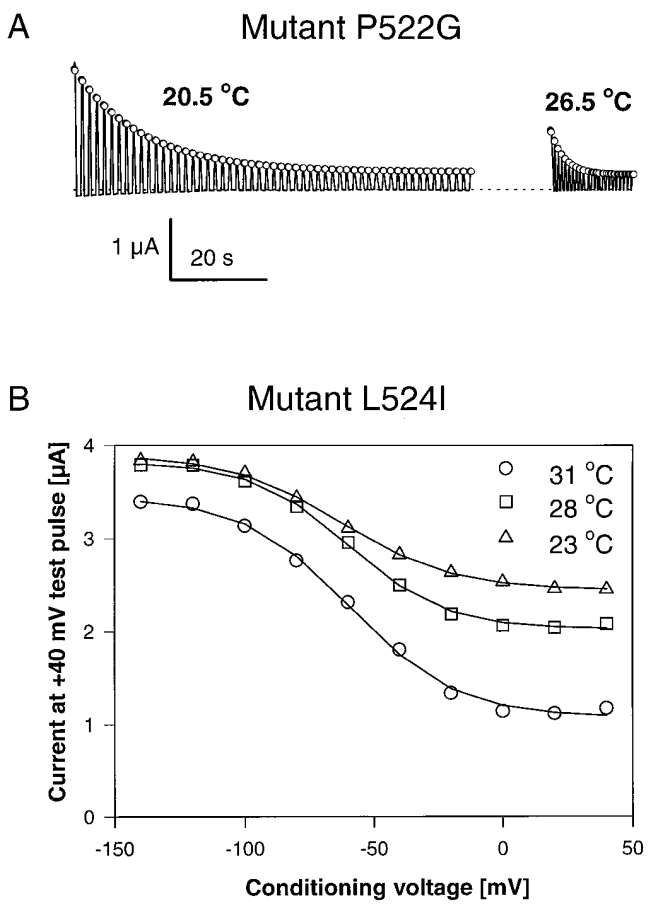

FIGURE 11. Mutants with altered slow gate. Time course of deactivation of the slow gate is shown for mutant P522G (*A*) and steady-state $p_{open}^{slow}(V)$ for mutant L524I (*B*) at the indicated temperatures.

two of its mutants. Fast gating kinetics show a moderate temperature dependence characterized by an activation enthalpy of 51 kJ/mole, corresponding to a Q_{10} of 2.2. This value was not changed when currents were measured under conditions where 80 mM extracellular chloride were replaced by iodide despite a slowed deactivation under these conditions.

Steady-state voltage dependence ($p_{open}^{fast}(V)$) was only slightly dependent on temperature. This would imply that opening and closing transitions have, more or less, the same temperature dependence. Thus, neither the open state nor the closed state seem to have a more ordered structure. More detailed measurements are, however, necessary to firmly establish such a conclusion.

If a simple diffusion-limited blocking mechanism (e.g., by intracellular OH^-) were responsible for fast gating, a Q_{10} of ~1.3–1.6, a value characteristic for diffusion, could be expected, at least for the on-rate of the block. Based on the observed value of $Q_{10} = 2.2$ it is not possible to rule out completely a blocking mechanism for the closing of the channel. A "true" conformational change is postulated within the simple gating model of Pusch et al. (1995*a*) in which intrinsic voltage-independent conformational changes are linked to external chloride concentration and transmembrane voltage by voltage-dependent binding of chloride within the channel pore.

In contrast to the fast gate, kinetics of slow gating is extremely temperature sensitive. The temperature dependence of WT deactivation kinetics is characterized by an apparent activation enthalpy of 260 kJ/mol, corresponding to a Q_{10} of ~40. We are not aware of any other biological process with a similarly large temperature dependence of kinetics. However, in a recent study, Ebihara (1996) found a high temperature sensitivity ($Q_{10} \sim 20$) of the magnitude of currents in *Xenopus* oocytes that are due to hemi-gap-junctional channels. The high Q_{10} was related to the assembly of connexins to a functional hemi-gap-junction. In our case, the high Q_{10} of 40 of the kinetics of the slow gate suggests that in order to move from an open slow gate to a closed slow gate the channel has to undergo a complex rearrangement; that is, some transition state has to differ greatly in its structure from either "ground" state. Also, steady-state voltage dependence of the slow gate (p_{open}^{slow}) is dependent on temperature in a characteristic way: Whereas the voltage of half maximal activation ($V_{1/2}^{slow}$) is relatively insensitive, the degree of maximal activation, but also the degree of minimal activation ("offset") is decreased by increasing temperature (Fig. 6). In addition, we noticed a correlation of the degree of minimal activation with the amount of ClC-0 expression (Fig. 5). The effects of temperature on the slow gate were confirmed at the single channel level. In addition, the patch experiments allow a quantitative measure of the open probability. They show that p_{open}^{slow} approaches unity at negative voltages and low temperatures.

The properties of the slow gate can be qualitatively described by the model shown in Fig. 10 *E*. For the following reasons at least four different states have to be postulated. If at least one voltage-dependent step is assumed with exponential voltage dependence, one has to postulate the existence of at least two open states. Otherwise, at some extreme voltage, all channels would have to be either fully closed or fully open, independent of temperature (as in the models shown in Fig. 10, *A*, *B*, and *D*). In contrast to this, we observe a temperature-dependent maximal and minimal activation of the slow gate. The same argument holds for any closed state (i.e., Fig. 10 *C*). Thus, the minimal model capable of describing the properties of the slow gate contains two open and two closed states. The scheme shown in Fig. 10 *E* represents one possible arrangement of two open and two closed states. Assuming only four states and exponential voltage dependence of rate constants, several features of the model can be deduced from the data. First, the main voltage dependence cannot be as-

sociated with $C_1 \leftrightarrow O_1$ and $C_2 \leftrightarrow O_2$ transitions, because this would drive the slow gate fully open or fully closed at extreme voltages. This leads to the assignment of the voltage-dependence to the transitions $C_1 \leftrightarrow C_2$ and $O_1 \leftrightarrow O_2$. Second, the main (steady-state) temperature dependence has to be assigned to the transitions $C_1 \leftrightarrow O_1$ and $C_2 \leftrightarrow O_2$. This can be concluded from the observation that, at (for example) positive voltages, where the channels are almost exclusively in states C_1 and O_1, increasing the temperature leads to a decrease in steady-state open probability. The same holds true for very negative voltages, where channels are predominantly in states C_2 and O_2. Third, the relative insensitivity of the "half-maximal voltage," $V_{1/2}^{slow}$, to temperature implies that the voltage-dependent steps are not strongly temperature sensitive (in the steady state).

On the other hand, it cannot be decided from the data which transitions are rate limiting and are associated with the high activation barrier that leads to the high Q_{10} of 40. However, because the enthalpy difference between two states is given by the difference of the activation enthalpy of the forward transition and the backward transition, we think that it is more likely that higher activation enthalpies are associated with the transitions between states which have a larger enthalpy difference. Thus we speculate that the rate-limiting transitions in the scheme of Fig. 10 *E* are the ones connecting open and closed states. This assumption has to be tested, however, in future experiments.

Several point mutations of ClC-0 that had been described by Ludewig et al. (1996*a*) drastically accelerated deactivation of the slow gate (e.g., L521I, P522G). In addition, for some of the mutations, the characteristics of the slow gate were difficult to measure, because of an increased offset in the steady-state p_{open}^{slow} (e.g., L524I, P525G). These large effects are clearly related to the strong temperature dependence of the slow gate. As shown by our measurements, the fast decaying mutant P522G is, at room temperature, very similar to WT that has been heated by some degrees.

A double-barreled model has been proposed for ClC-0 channels (Miller, 1982; Miller and White, 1984). Two identical protochannels gate independently from each other in a voltage-and anion-concentration–dependent manner (fast gate). Both protochannels are closed simultaneously by the common slow gate. The very large temperature dependence of slow gating kinetics and the dependence of the fraction of noninactivating channels on the amount of expressed currents are, in a vague way, compatible with an involvement of the slow gate in subunit interaction. From coexpression experiments with dominant negative mutations Steinmeyer et al. (1994) concluded that the homologous chloride channel ClC-1 is a functional homomer with more than three, possibly four subunits. In contrast to this, Middleton et al. (1994) concluded from their sucrose gradient experiments that ClC-0 is probably a dimer. Also, recent functional analysis of dimeric ClC-0 constructs (Ludewig et al., 1996*b*) and coexpression studies (Middleton et al., 1996) point to a dimeric structure of ClC-0 with one subunit forming a single protopore. With a point mutation that abolished the voltage dependence of slow gating (S123T), Ludewig et al. (1996*b*) also demonstrated that slow gating of ClC-0 is a function of both subunits. Also chimerae in the COOH-terminal part change slow gating suggesting a role of this part of the protein in the slow gating mechanism (Fong and Jentsch, 1996). Definitely, more experiments are needed to establish the precise relation of the subunit composition to the double-barreled model and to the slow gate.

In summary, temperature has only mild effects on fast gating ($Q_{10} = 2.2$), compatible with a structurally very simple conformational change, whereas slow gating shows a very strong temperature dependence ($Q_{10} \sim 40$), pointing to a very complex structural rearrangement connected with this gate. In addition, the temperature dependence of $p_{open}^{slow}(V)$ clearly shows that the slow gate has to be described by at least two open and two closed states.

We thank Christine Neff for expert technical assistance.

This work was supported by grants of the Deutsche Forschungsgemeinschaft.

Original version received 3 July 1996 and accepted version received 27 September 1996.

REFERENCES

Bauer, C.K., K. Steinmeyer, J.R. Schwarz, and T.J. Jentsch. 1991. Completely functional double-barrelled chloride channels expressed from a single *Torpedo* cDNA. *Proc. Natl. Acad. Sci. USA*. 88: 11052–11056.

Becker, P.E. 1973. Generalized non-dystrophic myotonia. The dominant (Thomsen) type and the recently identified recessive type. *In* New Developments in Electromyography. J.E. Desmedt, editor. S. Karger, Basel. 407–412.

Ebihara, L. 1996. *Xenopus* connexin38 forms hemi-gap-junctional channels in the nonjunctional plasma membrane of *Xenopus* oocytes. *Biophys. J.* 71:742–748.

Fisher, S.E., G.C.M. Black, S.E. Lloyd, E. Hatchwell, O. Wrong, R.V. Thakker, and I.W. Craig. 1994. Isolation and partial characterization of a chloride channel gene which is expressed in kidney and

is a candidate for Dent's disease (an X-linked hereditary nephrolithiasis). *Hum. Mol. Genet.* 3:2053–2059.

Fong, P., and T.J. Jentsch. 1996. Elimination of ClC-0 slow gating. *Biophys. J.* 70:A8. (Abstr.).

Hamill, O.P., A. Marty, E. Neher, B. Sakmann, and F.J. Sigworth. 1981. Improved patch-clamp techniques for high-resolution current recording from cells and cell-free membrane patches. *Pflüg. Arch. Eur. J. Physiol.* 391:85–100.

Hanke, W., and C. Miller. 1983. Single chloride channels from *Torpedo* electroplax. Activation by protons. *J. Gen. Physiol.* 82:25–42.

Jentsch, T.J. 1996. Chloride channels: a molecular perspective. *Curr. Opin. Neurobiol.* 6:303–310.

Jentsch, T.J., W. Günther, M. Pusch, and B. Schwappach. 1995*a*. Properties of voltage-gated chloride channels of the ClC gene family. *J. Physiol. (Lond.).* 482P:19S–25S.

Jentsch, T.J., C. Lorenz, M. Pusch, and K. Steinmeyer. 1995*b*. Myotonias due to ClC-1 chloride channel mutations. *In* Ion Channels and Genetic Diseases, Vol. 50 of Society of General Physiologist Series. D.C. Dawson and R.A. Frizzell, editors. Rockefeller University Press, New York. 149–159.

Jentsch, T.J., K. Steinmeyer, and G. Schwarz. 1990. Primary structure of *Torpedo marmorata* chloride channel isolated by expression cloning in *Xenopus* oocytes. *Nature (Lond.).* 348:510–514.

Koch, M.C., K. Steinmeyer, C. Lorenz, K. Ricker, F. Wolf, M. Otto, B. Zoll, F. Lehmann-Horn, K.-H. Grzeschik, and T.J. Jentsch. 1992. The skeletal muscle chloride channel in dominant and recessive human myotonia. *Science (Wash. DC).* 257: 797–800.

Lloyd, S.E., S.H.S. Pearce, S.E. Fisher, K. Steinmeyer, B. Schwappach, S.J. Scheinmann, B. Harding, A. Bolino, M. Devoto, P. Goodyer, et al. 1995. Mutations in the chloride channel ClC-5 are associated with X-linked hypercalciuric nephrolithiasis. *Nature (Lond.).* 379:445–449.

Ludewig, U., T.J. Jentsch, and M. Pusch. 1996*a*. Analysis of a protein region involved in permeation and gating of the voltage-gated chloride channel ClC-0. *J. Physiol. (Lond.).* In press.

Ludewig, U., M. Pusch, and T.J. Jentsch. 1996*b*. Two physically distinct pores in the dimeric ClC-0 chloride channel. *Nature (Lond.).* 383:340–343.

Methfessel, C., V. Witzemann, T. Takahashi, M. Mishina, S. Numa, and B. Sakmann. 1986. Patch clamp measurements on *Xenopus laevis* oocytes: currents through endogenous channels and implanted acetylcholine receptor and sodium channels. *Pflüg. Arch. Eur. J. Physiol.* 407:577–588.

Middleton, R.E., D.J. Pheasant, and C. Miller. 1994. Purification reconstitution, and subunit composition of a voltage-gated chloride channel from *Torpedo* electroplax. *Biochemistry.* 33:13189–13198.

Middleton, R.E., D.J. Pheasant, and C. Miller. 1996. Homodimeric architecture of a ClC-type Cl^- channel. *Nature (Lond.).* 383:337–340.

Miller, C. 1982. Open-state substructure of single chloride channels from *Torpedo* electroplax. *Philos. Trans. R. Soc. Lond. B.* 299:401–411.

Miller, C., and M.M. White. 1984. Dimeric structure of single chloride channels from *Torpedo* electroplax. *Proc. Natl. Acad. Sci. USA.* 81:2772–2775.

Pusch, M., and T.J. Jentsch. 1994. Molecular physiology of voltage-gated chloride channels. *Physiol. Rev.* 74:813–827.

Pusch, M., U. Ludewig, A. Rehfeldt, and T.J. Jentsch. 1995*a*. Gating of the voltage-dependent chloride channel ClC-0 by the permeant anion. *Nature (Lond.).* 373:527–531.

Pusch, M., K. Steinmeyer, M.C. Koch, and T.J. Jentsch. 1995*b*. Mutations in dominant human myotonia congenita drastically alter the voltage-dependence of the ClC-1 chloride channel. *Neuron.* 15:1455–1463.

Rychkov, G.Y., M. Pusch, D.S.J. Astill, M.L. Roberts, T.J. Jentsch, and A.H. Bretag. 1996. Concentration and pH dependence of skeletal muscle chloride channel ClC-1. *J. Physiol. (Lond.).* In press.

Smith, R.L., G.H. Clayton, C.L. Wilcox, K.W. Escuro, and K.J. Staley. 1995. Differential expression of an inwardly rectifying chloride conductance in rat brain neurons: a potential mechanism for cell-specific modulation of postsynaptic inhibition. *J. Neurosci.* 15:4057–4067.

Steinmeyer, K., R. Klocke, C. Ortland, M. Gronemeier, H. Jokusch, S. Gründer, and T.J. Jentsch. 1991*a*. Inactivation of muscle chloride channel by transposon insertion in myotonic mice. *Nature (Lond.).* 354:304–308.

Steinmeyer, K., C. Lorenz, M. Pusch, M.C. Koch, and T.J. Jentsch. 1994. Multimeric structure of ClC-1 chloride channels as revealed by mutations in dominant myotonia congenita (Thomsen). *EMBO (Eur. Mol. Biol. Organ.) J.* 13:737–743.

Steinmeyer, K., C. Ortland, and T.J. Jentsch. 1991*b*. Primary structure and functional expression of a developmentally regulated skeletal muscle chloride channel. *Nature (Lond.).* 354:301–304.

Steinmeyer, K., B. Schwappach, M. Bens, A. Vandewalle, and T.J. Jentsch. 1995. Cloning and functional expression of rat ClC-5, a chloride channel related to kidney disease. *J. Biol. Chem.* 270: 31172–31177.